Article

Photoinduced Reorganization of Motor-Doped Chiral Liquid Crystals: Bridging Molecular Isomerization and Texture Rotation

Alessandro Bosco, Mahthild G. M. Jongejan, Rienk Eelkema, Nathalie Katsonis, Emmanuelle Lacaze, Alberta Ferrarini, and Ben L. Feringa

J. Am. Chem. Soc., **2008**, 130 (44), 14615-14624 • DOI: 10.1021/ja8039629 • Publication Date (Web): 08 October 2008

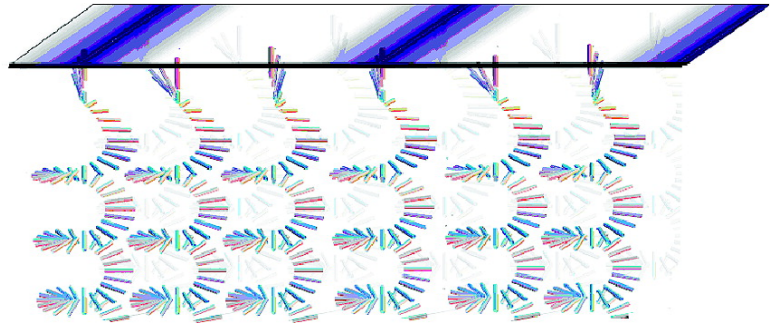

J|A|C|S
ARTICLES

Published on Web 10/08/2008

Photoinduced Reorganization of Motor-Doped Chiral Liquid Crystals: Bridging Molecular Isomerization and Texture Rotation

Alessandro Bosco,[†,¶] Mahthild G. M. Jongejan,[‡] Rienk Eelkema,[‡,#] Nathalie Katsonis,[*,‡,⊥] Emmanuelle Lacaze,[*,§] Alberta Ferrarini,[*,†] and Ben L. Feringa[*,‡]

Dipartimento di Scienze Chimiche, Università di Padova, Via Marzolo 1, 35131 Padova, Italy, Department of Organic and Molecular Inorganic Chemistry, Stratingh Institute for Chemistry, University of Groningen, Nijenborgh 4, 9747 AG Groningen, The Netherlands, Institut des Nano-Sciences de Paris, CNRS-UMR7588, Université Pierre et Marie Curie, Campus Boucicaut, 140 rue de Lourmel 75015 Paris, France, and CEMES, CNRS, University of Toulouse, 29 rue J. Marvig, 31055 Toulouse Cedex 4, France

Received May 27, 2008; E-mail: katsonis@cemes.fr; emmanuelle.lacaze@insp.jussieu.fr; alberta.ferrarini@unipd.it; b.l.feringa@rug.nl

Abstract: We recently reported that the photoisomerization of molecular motors used as chiral dopants in a cholesteric liquid crystal film induces a rotational reorganization which can be observed by optical microscopy and produces the motion of microscopic objects placed on top of the film (Feringa, B. L.; et al. *Nature* **2006**, *440*, 163; *J. Am. Chem. Soc.* **2006**, *128*, 14397). The mechanism underlying the mesoscopic manifestation of the molecular process was not fully understood, and here we present a joint theoretical and experimental investigation, which provides a detailed insight into the mechanism of texture rotation. This description allows us to identify the interplay between the chemical structure of the chiral dopant and the material properties of the liquid crystal host, and to quantify their role in the observed dynamic phenomenon. We have found that a crucial role is played by the hybrid anchoring of the liquid crystal, with the director parallel to the substrate and perpendicular to the interface with air; in this configuration an almost unperturbed cholesteric helix, with its axis normal to the substrate, is present in most of the film, with strong deformations only close to the free interface. The texture rotation observed in the experiment reflects the rotation of the director during the unwinding of the cholesteric helix, produced by the change in shape of the chiral dopant under photoisomerization. The rotational reorganization is controlled by the photochemical process, via the coupling between the chirality of the dopant and the elastic properties of the liquid crystal host.

Introduction

Liquid crystals (LCs) find large-scale applications in LC displays and are promising materials for the induction of meso- or macroscale dynamics under molecular control, because of their sensitivity to external stimuli (temperature, electric and magnetic fields), coupled to their intrinsic fluidity.[1] Particularly interesting effects have been found in the case of chiral mesophases. For example, rotation of drops of cholesteric LCs induced by external fields of various nature has been observed.[2] In the early 20th century, Lehmann discovered that a thermal gradient along the helical axis can result in a continuous rotation of a cholesteric drop.[3] Later, analogous effects were found in the presence of an electric field[4] and under a concentration gradient of chiral solutes parallel to the helix axis.[5] A general interpretation for these phenomena can be given, based on the lack of mirror symmetry in cholesteric LCs.[3,6]

The doping of an achiral nematic LC host with chiral, nonracemic molecules induces the formation of a cholesteric mesophase.[7] By using bistable dopants, it is possible to achieve photocontrol of the pitch of the cholesteric mesophase.[8] In particular, some of us recently reported that the photoisomer-

[†] Università di Padova.
[¶] Present address: International School for Advanced Studies (SISSA), Via Beirut 2-4, 34014 Trieste, Italy.
[‡] University of Groningen.
[⊥] University of Toulouse.
[§] Université Pierre et Marie Curie.
[#] Present Address: University of Delft, Julianalaan 136, 2628BL Delft, The Netherlands.

(1) (a) De Gennes P. G.; Prost, J. *The Physics of Liquid Crystals*, 2nd ed.; Oxford University Press: Oxford, 1993. (b) Vertogen, G.; de Jeu, W. H. *Thermotropic Liquid Crystals, Fundamentals*; Springer Series in Chemical Physics *45*; Springer-Verlag: Berlin, 1988. (c) Mitov, M. *Les cristaux liquides*; Presses Universitaires de France: Paris, 2000; Collection "Que Sais-Je?", no. 1296.
(2) (a) Chandrasekhar, S. *Liquid Crystals*, 2nd ed.; Cambridge University Press: Cambridge, 1992. (b) Oswald, P.; Pieranski. P. *Nematic and Cholesteric Liquid Crystals: Concepts and Physical Properties Illustrated by Experiments*; Taylor & Francis Ltd.: London, 2005.
(3) Lehmann, O. *Ann. Phys. (Weinheim)* **1900**, *2*, 649–705.
(4) (a) Madhusudana, N. V.; Pratibha, R. *Mol. Cryst. Liq. Cryst.* **1989**, *5*, 1827–1840. (b) Madhusudana, N. V.; Pratibha, R.; Padmini, H. P. *Mol. Cryst. Liq. Cryst.* **1991**, *202*, 35–49.
(5) Gvozdovskyy, I.; Terenetskaya, I. *Liq. Cryst. Today* **2002**, *11*, 8–12.
(6) Brand, H. R.; Pleiner, H. In *Encyclopedia of Materials: Science and Technology*; Buschow, K. H. J., Cahn, R., Flemings, M. C., Ilschner, B., Kramer, E. J., Mahajan, S., Veyssiere P., Eds.; Elsevier: Amsterdam, 2001.

ization of molecular motors[9] used as chiral dopants in LC films induces a rotational reorganization of the texture of the mesophase, which can be observed by optical microscopy.[10,11] The process is reversible: under UV irradiation the rotation of the texture proceeds until the photostationary state (PSS) is reached; once UV irradiation is stopped, the initial state is restored by rotation in the opposite direction. The origin of the phenomenon lies in the fact that the ability of the dopant to twist the nematic LC host changes upon photoisomerization. However, the connection between the molecular isomerization and the observed modifications in the texture remained unclear, which prevented the elucidation of such features as the correlation between the dopant chirality and the sense of rotation.

As cholesteric materials are used as tunable bandpass filters, reflectors or polarizers,[12] temperature or pressure sensors, and in biomedical research,[13] the actuator properties revealed by semifree films of motor-doped LCs could open the way to innovative applications. In order to guide future design of motor-doped LCs, it will be necessary to control the rotational behavior of these systems: the speed of rotation, the modification of period of the fingerprints, the geometry of the texture, etc. In this contribution, we present a detailed rationalization for the rotational reorganization of motor-doped LC films, by elucidating the relation between the isomerization of the motors and the rotation of the texture.

Several molecules have been used as switchable chiral dopants in LCs, e.g., azobenzenes, diarylethenes, fulgides, and molecular motors, which belong to the family of overcrowded alkenes.[7] These molecules undergo isomerization upon irradiation with UV light, and, as a consequence, their shape is modified, along with their ability to twist the nematic LC host. Overcrowded alkene-based molecular motors and switches have been shown to be particularly efficient chiral dopants for inducing cholesteric ordering in nematic LCs.[14,15] In this study we shall focus on the phenyl substituted molecular motor **1** shown in Scheme 1. This motor's kinetic behavior and isomerization processes are well understood:[16] upon photoisomerization of the central olefinic bond (the axis of rotation), the stable isomer (*P*)-**1a**, with **P** helicity, undergoes an inversion of molecular helicity leading to the unstable form (*M*)-**1b**, with

Scheme 1. Unidirectional Rotary Cycle for the Molecular Motor

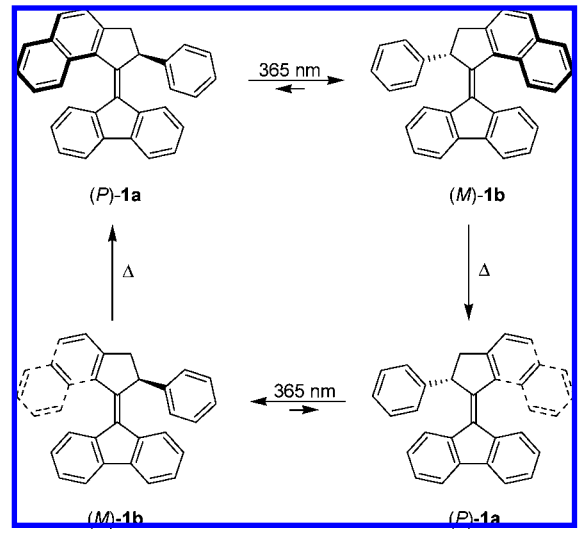

M helicity.[17] At the same time, the phenyl substituent adopts, instead of pseudoaxial, the more strained pseudoequatorial orientation. Through release of this strain, a thermal inversion of molecular helicity occurs, resulting in the (*P*)-**1c** structure, which is indistinguishable from (*P*)-**1a** in this particular case, as the "lower half" of this motor is symmetrical. The combined photochemical and thermal isomerization step completes the first half of a 360° rotary cycle of the "upper half" rotor with respect to the "lower half" stator part of **1**.

As in our previously reported experiments,[10,11] the molecular motor **1** was dissolved in E7, the components of which are shown in Figure 1. E7 is a nematic, achiral LC mixture; at room temperature, the elongated molecules are distributed without positional order but they are preferentially aligned along a given direction, usually referred to as the *director*. The introduction of the chiral dopant results in the helical twist of the director. The cholesteric mesophase thus generated is characterized by the pitch (p) of the helix, which is defined as the length corresponding to a 360° rotation of the director. The pitch depends on the structure of the chiral dopant, its concentration, and its enantiomeric excess. Under high dilution, a linear relationship is observed between the concentration of the dopant and the inverse of the cholesteric pitch. The ability of a given chiral dopant to twist the nematic host is quantified by its *helical twisting power* (HTP), defined as

$$\mathrm{HTP} = \frac{1}{\mathrm{ee}\, c\, p} \tag{1}$$

where c is the concentration (expressed as mole fraction), p is the cholesteric pitch, and ee is the enantiomeric excess.

By convention, the pitch p can be positive or negative, with the sign indicating the handedness of the cholesteric helix (right- and left-handed, respectively). In the case of a mixture of dopants, the resulting HTP is the sum of individual contributions:

$$\mathrm{HTP} = \sum_i x_i \,\mathrm{HTP}_i \tag{2}$$

(7) For reviews on LC dopants, see, e.g.: (a) Spada, G. P.; Proni, G. *Enantiomer* **1998**, *3*, 301–314. (b) Eelkema, R.; Feringa, B. L. *Org. Biomol. Chem.* **2006**, *4*, 3729–3745.
(8) See, for example: (a) Ikeda, T. *J. Mater. Chem* **2003**, *13*, 2037–2057, and references therein. (b) Pieraccini, S.; Gottarelli, G.; Labruto, R.; Masiero, S.; Pandoli, O.; Spada, G. P. *Chem. Eur. J.* **2004**, *10*, 5632–5639. (c) Li, Q.; Green, L.; Venkataraman, N.; Shiyanovskaya, I.; Khan, A.; Urbas, A.; Doane, J. W. *J. Am. Chem. Soc.* **2007**, *129*, 12908–12909.
(9) (a) Feringa, B. L. J. *Org. Chem.* **2007**, *72*, 6635–6652. (b) Browne, W. R.; Feringa, B. L. *Nat. Nanotechnol.* **2006**, *1*, 25–35.
(10) Eelkema, R.; Pollard, M. M.; Vicario, J.; Katsonis, N.; Ramon, B. S.; Bastiaansen, C. W. M.; Broer, D. J.; Feringa, B. L. *Nature* **2006**, *440*, 163.
(11) Eelkema, R.; Pollard, M. M.; Katsonis, N.; Vicario, J.; Broer, D. J.; Feringa, B. L. *J. Am. Chem. Soc.* **2006**, *128*, 14397–14407.
(12) Mitov, M.; Dessaud, N. *Nat. Mater.* **2006**, *5*, 361–364.
(13) Woltman, S. J.; Jay, G. D.; Crawford, G. P. *Nat. Mater.* **2007**, *6*, 929–938.
(14) van Delden, R. A.; Koumura, N.; Harada, N.; Feringa, B. L. *Proc. Natl. Acad. Sci. U.S.A.* **2002**, *99*, 4945–4949.
(15) Pijper, D.; Jongejan, M. G. M.; Meetsma, A.; Feringa, B. L. *J. Am. Chem. Soc.* **2008**, *130*, 4541–4552.
(16) (a) Vicario, J.; Meetsma, A.; Feringa, B. L. *Chem. Commun.* **2005**, 5910–5912. (b) Vicario, J.; Walko, M.; Meetsma, A.; Feringa, B. L. *J. Am. Chem. Soc.* **2006**, *128*, 5127–5135.
(17) Eliel, E. L.; Wilen, S. H. *Stereochemistry of Organic Compounds*; Wiley: New York, 1994.
(18) Raynes, P.; Tough, R. J. A.; Davies, K. A. *Mol. Cryst. Liq. Cryst.* **1979**, *56*, 63–68.

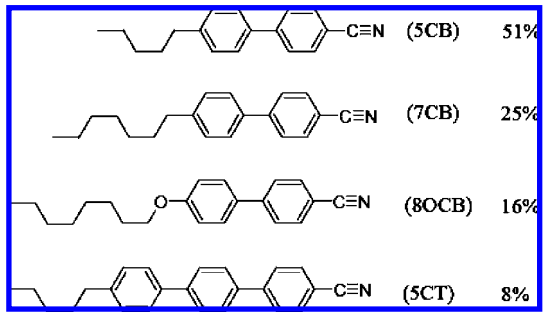

Figure 1. Composition of the liquid crystal mixture E7 (isotropic−nematic transition temperature $T_{NI} = 334$ K, average molecular weight $M = 271.2$ g mol^{-1}).[18]

Figure 2. Director configurations in a cholesteric LC film under different anchoring conditions at the two boundaries. The rods represent the orientation of the director. (Left) The axis of the cholesteric helix is perpendicular to the glass plate, as in planar−planar (PP) anchoring. (Right) The cholesteric axis is parallel to the glass plate, as in homeotropic−homeotropic (HH) anchoring.

where x_i is the fraction of i isomer ($\sum_i x_i = 1$) and HTP_i is the corresponding helical twisting power. The chiral dopant (*P*)-**1a** has been found experimentally to have high and positive HTP; an opposite twisting ability of the (*M*)-**1b** isomer can be inferred from the negative HTP value measured when the PSS is reached.[9] However, the exact isomer population at PSS is not known in the LC phase due to experimental restrictions.[10,11]

The cholesteric texture observed by optical microscopy under crossed polarizers reflects the transmittance of the film, which depends on the configuration of the director within it, and is influenced by the boundary conditions (see Figure 2).[2b,19] When the director of a cholesteric LC is anchored under planar boundary conditions at both interfaces (PP anchoring), i.e., with the long molecular axis parallel to the glass plates, the axis of the cholesteric helix orients perpendicular to the glass plates. The corresponding texture is characterized by the so-called "oily streaks".[19] Alternatively, a fingerprint texture is observed in the presence of homeotropic−homeotropic (HH) anchoring, when the axis of the helix is parallel to the glass plates. A less investigated organization is obtained when the cholesteric LC is submitted to hybrid anchoring (PH), i.e., planar unidimensional anchoring on one side (P) and homeotropic on the other side (H). Such a configuration also leads to the formation of a fingerprint pattern,[20] as observed in our previous investigations.[10,11] In the present study we will provide evidence that, in the experimental conditions we used, the chirally doped E7 film presents a geometry of hybrid anchoring.

Results and Discussion

In the frame of our multiscale analysis of rotational reorganization, we shall start from the characterization of the chiral

(19) Dierking, I. *Textures of Liquid Crystals*; Wiley-VCH: Weinheim, 2003.
(20) Baudry, J.; Brazovskaia, M.; Lejcek, L.; Oswald, P.; Pirkl, S. *Liq. Cryst.* **1996**, *21*, 893–901.

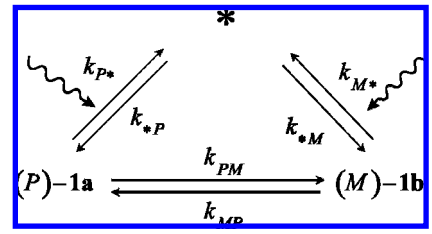

Figure 3. Photochemical and thermal isomerization processes undergone by the molecular motor **1**. The asterisk is used to represent, in a generic way, the excited state.

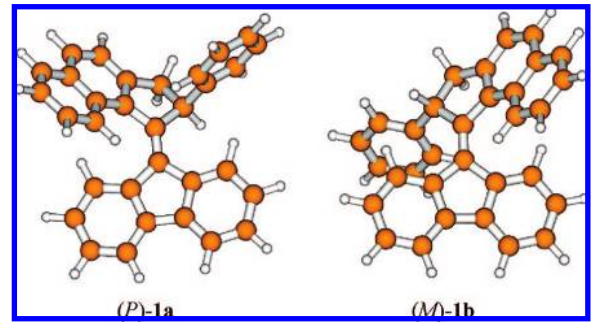

Figure 4. Geometry of the stable isomer of (*P*)-**1a** (left) and the unstable isomer (*M*)-**1b** (right), as obtained from geometry optimization (DFT/B3LYP/6-31g**).[21]

dopant **1**, considering first the isomerization process and then the orientational order of the two isomers in the nematic host and their shape chirality, both of which determine their ability to twist the director in the nematic phase. We shall then describe the configuration of the director in the doped LC film, which depends on the anchoring conditions, and finally the dynamics of its reorganization, in connection with the isomerization of the dopant.

Kinetics of Isomerization. Under irradiation with UV light, the molecular motor **1** undergoes the processes schematically shown in Figure 3; here a generic excited state has been considered, without going into the details of the excited-state dynamics, which are not known.

Figure 4 shows the geometry of the stable isomer (*P*)-**1a** and the unstable isomer (*M*)-**1b** of the chiral dopant, as obtained from DFT calculations at the B3LYP/6-31g** level.[21] The geometry of (*P*)-**1a** is very similar to that obtained from the X-ray structure.[16] The figure shows that, as far as the fluorene ("lower half") and naphthyl moieties ("upper half") are concerned, the two isomers are nearly mirror images of each other, with the naphthyl plane twisted on opposite sides in the two cases. The quantum mechanical analysis of the saddle point along the isomerization pathway shows that the isomerization process involves the concerted displacement of several atoms.[21]

If the decay rates from the excited state (k_{*M} and k_{*P}) are much faster than the other rates (k_{MP}, k_{PM}, k_{P*}, and k_{M*}), then the population in the excited state is negligible ($x_* \sim 0$), and the time evolution of x_P and x_M, the fraction of stable isomer (*P*)-**1a** and unstable (*M*)-**1b**, respectively, after the UV light has been switched on, can be approximated as

$$x_P(t) \approx x_{P,PSS} + (x_{M,PSS}x_{P,eq} - x_{P,PSS}x_{M,eq})\, e^{-t/\tau_{photo}} \quad (3a)$$

$$x_M(t) \approx x_{M,PSS} - (x_{M,PSS}x_{P,eq} - x_{P,PSS}x_{M,eq})\, e^{-t/\tau_{photo}} \quad (3b)$$

where a short and weak transient contribution has been neglected, and the characteristic time of photoisomerization has

been introduced:

$$\tau_{\text{photo}} \approx \left(k_{MP} + k_{PM} + \frac{k_{P*}k_{*M} + k_{M*}k_{*P}}{k_{*M} + k_{*P}} \right)^{-1} \quad (4)$$

The fractions, $x_{P,\text{PSS}}$ and $x_{M,\text{PSS}}$, of stable isomer (*P*)-**1a** and unstable isomer (*M*)-**1b**, respectively, at the PSS are linked by the relation

$$\frac{x_{M,\text{PSS}}}{x_{P,\text{PSS}}} \approx \frac{k_{P*}k_{*M} + k_{PM}(k_{*P} + k_{*M})}{k_{M*}k_{*P} + k_{MP}(k_{*P} + k_{*M})} \quad (5)$$

while those in the equilibrium state without UV light, $x_{P(M),\text{eq}}$, comply with the Boltzmann distribution,

$$\frac{x_{M,\text{eq}}}{x_{P,\text{eq}}} = \mathrm{e}^{-\Delta E_{MP}/k_{\text{B}}T} \quad (6)$$

with $\Delta E_{MP} = E_M - E_P$ being the potential energy difference between (*P*)-**1a** and (*M*)-**1b**.

When, starting from the PSS, irradiation with UV light is stopped, the equilibrium population is recovered according to the equations:

$$x_P(t) = x_{P,\text{eq}} + (x_{M,\text{eq}}x_{P,\text{PSS}} - x_{P,\text{eq}}x_{M,\text{PSS}})\, \mathrm{e}^{-t/\tau_{\text{therm}}} \quad (7a)$$

$$x_M(t) = x_{M,\text{eq}} - (x_{M,\text{eq}}x_{P,\text{PSS}} - x_{P,\text{eq}}x_{M,\text{PSS}})\, \mathrm{e}^{-t/\tau_{\text{therm}}} \quad (7b)$$

with the characteristic time of thermal isomerization,

$$\tau_{\text{therm}} = (k_{MP} + k_{PM})^{-1} \quad (8)$$

The kinetic constants appearing in Figure 3 can be estimated on the basis of experimental and theoretical considerations:

k_{P*} and k_{M*}, the kinetic constants for light absorption of (*P*)-**1a** and (*M*)-**1b**, depend on both the radiation energy density and the molar extinction coefficient of the dopant. Considering that under our experimental conditions the irradiation intensity is about one-fifth of the nominal value for the lamp used in the experiment (470 μW/cm^2),[22] given the molar extinction coefficient for (*P*)-**1a** at 365 nm ($\sim$11 000 dm^3 mol^{-1}cm^{-1}),[16] we can estimate $k_{P*} \approx 0.005$ s^{-1}.[21,23] The ratio between k_{P*} and k_{M*} is related to the ratio of molar extinction coefficients for the two isomers;[23] from the electronic absorption spectra of **1** in hexane at -20 °C,[16] the relation $k_{M*} \sim k_{P*}/10$ is derived.[24]

k_{*M} and k_{*P} are the kinetic constants for the decay from the excited state to either the (*P*)-**1a** or the (*M*)-**1b** isomer. In the literature, lifetimes of the order of hundreds of picoseconds have been reported for analogous systems;[25] therefore, we can assume that $k_{*P},k_{*M} \approx 10^{10}$ s^{-1}, but any more precise information is lacking.

k_{MP} and k_{PM}, the rate constants for direct (*P*)-**1a** $\rightarrow$ (*M*)-**1b** and (*M*)-**1b** $\rightarrow$ (*P*)-**1a** isomerizations, can be evaluated from measurements of the thermal isomerization rate, k_{therm}. According to the Kramers theory for the reaction rate in the condensed phase,[26] we can write for the (*M*)-**1b** $\rightarrow$ (*P*)-**1a** isomerization rate:

$$k_{MP} = \frac{\sqrt{|V_{\text{s}}|\,V_M}}{2\pi\xi_{\text{s}}} \exp\left[-\frac{\Delta E_{\text{s}}}{k_{\text{B}}T} \right] \quad (9)$$

where V_{s} and V_M are the second derivatives of the potential energy, respectively calculated at the saddle point and in the minimum corresponding to the (*M*)-**1b** isomer, ΔE_{s} is the barrier height, measured from the (*M*)-**1b** state, and ξ_{s} is the friction coefficient opposing the molecular motion involved by the reaction under investigation, evaluated in correspondence with the saddle point.[27] Assuming that the curvature of the potential energy is similar, in absolute value, for the (*P*)-**1a** and (*M*)-**1b** minima and using the energy difference $\Delta E_{MP} = 14$ kJ mol^{-1}, obtained for **1** by DFT calculations,[21] the ratio $k_{PM}/k_{MP} \approx 0.003$ can be estimated; therefore, we can approximate $\tau_{\text{therm}} \approx 1/k_{MP}$. The rate constant for thermal isomerization of **1** was obtained from CD experiments in hexane at room temperature: $1/\tau_{\text{therm}} \approx 1.18 \times 10^{-3}$ s^{-1}.[16] However, the value of τ_{therm} in E7 might be different, since the nematic host can affect the transition rate through the potential energy profile and through the friction coefficient, which is inversely proportional to the viscosity of the fluid, η. It is worth stressing that, in the case of LCs, the viscosity experienced by molecular motions will in general be different from that affecting the dynamics of the director; the former can be probed, e.g., by ESR spectra of paramagnetic solutes. ESR spectra of Tempone in E7 do not exhibit dramatic changes on going from the isotropic to the nematic phase;[28] from simulation of the ESR spectra at 300 K (nematic) and 345 K (isotropic), we have estimated the ratio $\eta^{300}/\eta^{345} \approx 4$. Considering that the viscosity of isotropic E7 at 345 K is likely to be higher than that of hexane at room temperature (0.3 cP),[29] a decrease of the rate constant in E7 can be expected, i.e., $k_{MP} < 10^{-3}$ s^{-1}.

From all these considerations, $\tau_{\text{therm}} > 1000$ s can be assumed for thermal isomerization of **1** in E7 at room temperature. For the photochemical process, on the basis of eq 4 and the considerations presented above, a value of τ_{photo} of the order of hundreds of seconds seems reasonable for our experimental conditions.

Orientational Order and Twisting Ability of the Chiral Dopant in the LC Host. Most properties of LCs are conveniently described in terms of the *director field* $\mathbf{n}(\mathbf{R})$, which is locally defined by the average orientation of the mesogens. The director introduces a relevant intermediate length-scale, between the molecular and the macroscopic levels, the behavior of which can be described by the continuum elastic theory: director deformation, over distances much longer than the molecular dimensions, is opposed by elastic restoring torques, as described by the Frank expression:[30]

(21) See details in the Supporting Information.
(22) Spectroline; Spectronics Corp.: Westbury, NY (http://www.spectroline.com/mineralogy_lamps_hand.html#table).
(23) Turro, N. J. *Modern Molecular Photochemistry*; University Science Books: Sausalito, CA, 1991.
(24) The molar extinction coefficients of the (*P*)-**1a** and (*M*)-**1b** isomers at $\lambda = 365$ nm are derived from the electronic absorption spectra of **1** in hexane at -20 °C, recorded in the absence of UV light and in PSS state (see ref14), assuming a Gaussian line shape for each isomer, with equal oscillator strengths. The latter assumption is in agreement with the similar values predicted for the two isomers by TD-DFT calculations; its use for the analysis of the absorption spectrum of **1** in the PSS state yields $x_{M,\text{PSS}} = 0.84$ and $x_{P,\text{PSS}} = 0.16$, close to the values derived from NMR experiments.
(25) (a) Schuddeboom, W.; Jonker, S. A.; Warman, J. M.; de Haas, M. P.; Vermeulen, M. J. W.; Jager, W. F.; de Lange, B.; Feringa, B. L.; Fessenden, R. W. *J. Am. Chem. Soc.* **1993**, *115*, 3286–3290. (b) Zijlstra, R. W. J.; van Duijnen, P.Th.; Feringa, B. L.; Steffen, T.; Duppen, K.; Wiersma, D. A. *J. Phys. Chem. A* **1997**, *101*, 9828–9836.
(26) Kramers, H. A. *Physica* **1940**, *7*, 284–304.
(27) (a) Moro, G. J.; Ferrarini, A.; Polimeno, A.; Nordio, P. L. In *Reactive and Flexible Molecules in Liquids*; Dorfmüller, Th., Ed.; Kluwer Academic Publishers: Amsterdam, 1989. (b) Ferrarini, A.; Nordio, P. L. *J. Chem. Soc., Faraday Trans.* **1992**, *88*, 1733–1746.
(28) Franco, L.; Ceola, S., unpublished data.
(29) Lide, D. R., Ed. *Handbook of Chemistry and Physics*; CRC: Cleveland, OH, 2003.

$$a_{el} = K_t q + \frac{1}{2}K_{11}s^2 + \frac{1}{2}K_{22}q^2 + \frac{1}{2}K_{33}b^2 \quad (10)$$

where a_{el} is the Helmholtz free energy density, and s, q, and b denote the three deformation modes, $s = \nabla\cdot\mathbf{n}$ (splay), $q = -\mathbf{n}\cdot(\nabla \times \mathbf{n})$ (twist), and $b = \mathbf{n} \times (\nabla \times \mathbf{n})$ (bend). The K_{ii}'s are the corresponding *elastic constants*, and K_t is the so-called *chiral strength*, which vanishes in an achiral sample. The equilibrium configuration of the director in the bulk corresponds to the minimum of the elastic free energy. A cholesteric LC is characterized by a helically twisted director, with wavenumber

$$q = 2\pi/p = -K_t/K_{22} \quad (11)$$

In doped cholesteric LCs, the chiral strength K_t depends on the concentration and nature of dopant. At low dopant concentration, we can assume K_t to be proportional to the dopant concentration and K_{22} equal to that of the nematic LC host; therefore, eq 1 for the HTP follows. For a mixture of the two isomers of the chiral dopant **1**, we can write $K_t = x_P K_{t,P} + x_M K_{t,M}$, where $K_{t,P(M)}$ is the chiral strength contribution from the (*P*)-**1a** and (*M*)-**1b** isomers; it follows that the HTP of the mixture is given by eq 2.

The *surface interaction* model provides an expression connecting the chiral strength to the structure of the dopant; the following expression is obtained for the HTP:[31]

$$\mathrm{HTP} = AQ \quad (12)$$

where Q is the so-called *surface chirality parameter*, which is specific of each chiral dopant, for a given LC host at a given temperature. A is a quantity that only depends on the host; it is defined as $A = N_A\xi/2\pi K_{22}v_m$, with N_A the Avogadro number, v_m the molecular volume of the LC host, and ξ the orienting strength, which is related to the degree of order of the LC host. It follows from the definition that the value of A for a given LC host is a function of temperature and depends on the structure of the LC host, mainly through the twist elastic constant; it can simply be taken as a scaling parameter when comparing calculated and experimental HTP values for different chiral dopants in the same LC host (common values of A are of the order of unity if HTP and Q are given in μm^{-1} and $Å^{-3}$, respectively).[32] The key property accounting for the twisting ability of a given dopant is the surface chirality parameter Q, which is proportional to the helicity of the molecular surface, averaged over all orientations in the nematic environment. Labeling as x and y the molecular axes that tend to lie perpendicular to the director, we can write[31,32]

$$Q = -6^{1/2}(Q_{xx} + Q_{yy})S_\perp + 6^{-1/2}(Q_{yy} - Q_{xx})\Delta S_\perp \quad (13)$$

where Q_{ii} is the helicity of the molecular surface along the ith axis, $S_\perp = (S_{xx} + S_{yy})/2$, and $\Delta S_\perp = (S_{xx} - S_{yy})$, S_{ii} being the *order parameter*, which specifies the degree of alignment of the ith molecular axis of the dopant with respect to the local director in the cholesteric phase. The S_{ii}'s are the principal values of the Saupe matrix,[33] with $-0.5 \le S_{ii} \le 1$; the molecular axes (i) define the principal alignment directions in the molecule. Positive and negative S_{ii} values mean that the corresponding axes tend to lie parallel and perpendicular to the director, respectively. The order parameters are identical for a molecule and its mirror image, while the Q_{ii} values, thus the chirality parameter Q, take opposite values for enantiomeric pairs. The meaning of eq 13 can be expressed in the following way: due to the fluid character of the LC, dopants can sample all orientations, with certain preferences described by the order parameters; differently oriented dopants promote twist of the nematic director of different magnitude and handedness, and the resulting twist is a weighted average over all possible orientations.

Table 1. Order Parameters of **1** (Obtained Giving the Orienting Strength the Value $\xi = 0.025$ $Å^{-2}$) and the Corresponding Diagonal Elements of the Chirality Tensor (**Q**) and Chirality Parameter Q[a]

		S_{ii}	Q_{ii} ($Å^3$)	Q ($Å^3$)
(*P*)-**1a**[b]	*x*	0.06	−17	+36
	y	−0.28	95	
	z	0.22	−77	
(*P*)-**1a**[c]	*x*	0.05	−19	+30
	y	−0.27	79	
	z	0.23	−59	
(*M*)-**1b**[b]	*x*	0.05	20	−37
	y	−0.28	−96	
	z	0.23	76	

[a] *x*, *y*, and *z* are the principal axes of the Saupe matrix. The measured HTP of (*P*)-**1a** is 90 μm^{-1}.[10,11] [b] Geometry from DFT calculations.[21] [c] Geometry from X-ray analysis.[16]

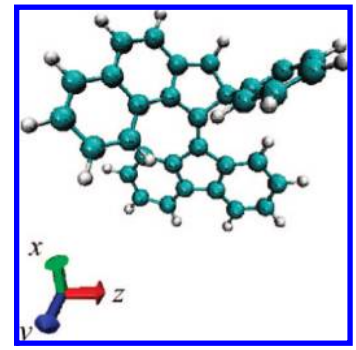

Figure 5. Principal alignment axes of the stable isomer (*P*)-**1a** in a nematic environment.

The Saupe matrix and chirality parameter have been calculated for the (*P*)-**1a** and (*M*)-**1b** isomers by assuming the geometry obtained from DFT calculations[21] and by using the X-ray structure available for the (*P*)-**1a** isomer.[16] The results are reported in Table 1. Figure 5 shows the principal alignment directions for the stable isomer, (*P*)-**1a**. The similarity of the order parameters for the stable and the unstable isomer indicates that they have essentially the same orientational behavior in the LC host. This behavior can be classified as disc-like: the *y* axis, roughly perpendicular to the fluorene plane, is predicted to preferentially orient normal to the local director; thus the director tends to lie on the fluorene plane, parallel to its long axis rather than perpendicular to it. It is worth stressing that a low order parameter along one single molecular direction, for example $S_{xx} \approx 0$ in the case of **1**, does not necessarily mean that, in a nematic LC host, the chiral dopant has a low degree of order. Actually, in case of **1**, the S_{yy} value indicates a fair degree of order of the motor, and the large difference between S_{xx} and S_{zz} corresponds to a significant anisotropy in the

(30) (a) Frank, F. C. *Discuss. Faraday Soc.* **1958**, *25*, 19–28. (b) Oseen, C. W. *Trans. Faraday Soc.* **1933**, *29*, 883–899.
(31) (a) Ferrarini, A.; Moro, G. J.; Nordio, P. L. *Phys. Rev. E* **1996**, *53*, 681–688. (b) Ferrarini, A.; Moro, G. J.; Nordio, P. L. *Mol. Phys.* **1996**, *87*, 485–499.
(32) Pieraccini, S.; Ferrarini, A.; Spada, G. P. *Chirality* **2008**, *20*, 749–759.
(33) Saupe, A. *Mol. Cryst. Liq. Cryst.* **1973**, *21*, 211–238.

alignment to the director of the fluorene plane. The calculated values of order parameters reported in Table 1 can be compared to experimental values determined by linear dichroism experiments. These provide the order parameter for the electronic transition dipole, according to the equation $S_{\mu\mu} = (A_{||} - A_{\perp})/(A_{||} + 2A_{\perp})$, where $A_{||}$ and $A_{\perp}$ are the absorbance parallel and perpendicular to the director, respectively.[34] The value $S_{\mu\mu} = 0.07$ has been obtained for a racemic mixture of **1** in K18 (*n*-hexyl-4,4′-cyanobiphenyl, $T_{NI} = 300$ K) at room temperature.[35] This value can be directly compared with the order parameters reported in Table 1 if we assume, in agreement with TD-DFT calculations,[21] that the transition dipole is approximately parallel to the central double bond, thus $S_{\mu\mu} \sim S_{xx}$.

We can see from Table 1 that the (*P*)-**1a** isomer is characterized by a high and positive Q_{yy} value, i.e., a strong and right-handed helicity along the axis that preferentially lies perpendicular to the local director; this explains the induction of a right-handed cholesteric helix. Similar results are obtained for the DFT-optimized[21] and the X-ray geometries:[16] the orientational behavior does not appear to be influenced by the small differences between the two structures. These differences have a slightly more pronounced influence on the chiral properties (Q_{ii}), which are very sensitive to geometry details, in particular to the twist angle between the aromatic units. In addition, we have calculated the twisting ability of the unstable state, which is not directly accessible by experiment: the Q_{ii} values obtained for (*M*)-**1b** are approximately the same as those for (*P*)-**1a**, but with opposite sign; correspondingly, $HTP_M \sim -HTP_P$ is predicted. This can be explained considering that the fluorene and the naphthyl moieties are twisted by approximately the same angle, but in opposite sense, in the two isomers. This behavior is analogous to that of binaphthyl.[31] Figure 6, where the contributions of the different molecular groups to the HTP of **1** are illustrated by colors,[36] shows that the strong twisting ability of the two isomers derives from the concordant effect of all the moieties, positive in the former case and negative in the other, with the only exception of the phenyl substituent.

Using the result $HTP_M \sim -HTP_P$ in eq 2, the isomer population in the PSS state in the cholesteric film can be calculated, given the HTP values measured with the Grandjean−Cano technique for the stable isomer (*P*)-**1a** (HTP = $+90\ \mu m^{-1}$) and for the PSS state (HTP < $-59\ \mu m^{-1}$) of **1**.[11] The value $x_{M,PSS} = 0.83$ is obtained, which is close to that derived from the previously mentioned ^{1}H NMR experiments in toluene at −40 °C, $x_{M,PSS} = 0.86$.[16]

Director Organization in the Cholesteric Film. The analysis presented in the previous section establishes a quantitative connection between the structure of the two isomers of molecular motor **1** and the director twist they induce in the cholesteric mesophase. However, this is not sufficient to explain the mesoscopic rotation observed under illumination. To this purpose, an insight into the director configuration in the semifree film of cholesteric LC is needed.

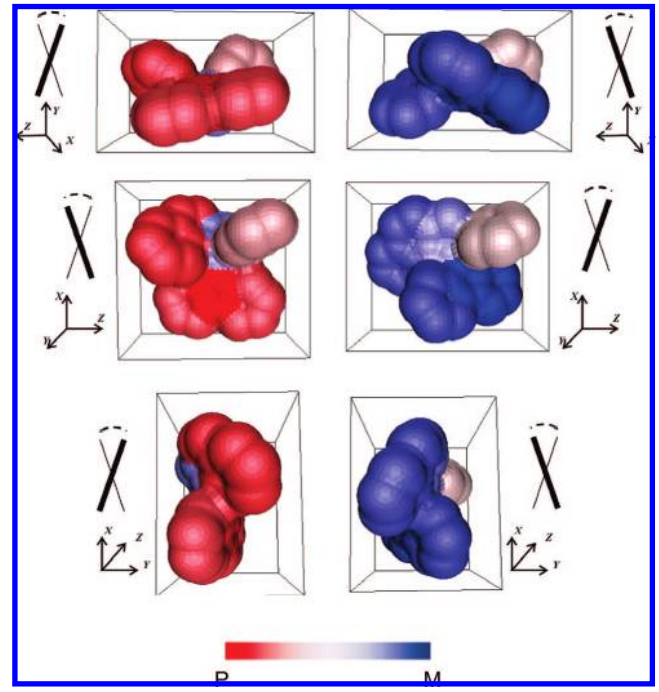

Figure 6. Views of the molecular surface of **1** along the principal alignment axes (left, (*P*)-**1a** isomer; right, (*M*)-**1b** isomer). The color code indicates the contribution to HTP of each functional group. At the side of each figure, the helicity of the molecule along the view axis is schematically represented as the angle between two rods.[37]

On rubbed polyimide, planar unidimensional anchoring of the cholesteric film can be safely assumed. In contrast, the anchoring geometry at the LC−air interface is less straightforward. For nematic films it has been reported that cyanobiphenyl groups, like those present in the E7 mixture, bearing a dipole of about 5 D, tend to orient with their main axis perpendicular to the interface.[38] Even less is known about the structure of semifree cholesteric LCs at the interface with air, but a subtle dependence on the interplay of elastic forces and surface tension has been reported.[39]

Our films of chirally doped E7 deposited on rubbed polyimide exhibit typical arch textures on areas where the thickness of the film varies (Figure 7). Locally, where the thickness of the sample is constant, the texture is characterized by parallel stripes. Under irradiation with UV light, these stripes rotate and their period is modified. Arch textures have been observed in wedge cells filled with a cholesteric LC with hybrid (PH) anchoring; both the period of the fingerprint texture and the orientation of the stripes constituting the fingerprint, with respect to the alignment direction on rubbed polyimide, were found to be dependent on the thickness of the cell.[20] This dependence is at the origin of arched textures when the thickness varies continuously. The structural similarities between the textures reported in ref20 and those observed in our experiments strongly suggest that the cholesteric film is likewise subjected to hybrid (PH) boundary conditions.

The following experiment more precisely shows that the rotation phenomenon we observed requires a hybrid anchoring geometry of the cholesteric film: a layer of E7 doped with **1**

(34) Dunmur, D.; Toriyama, K. In *Handbook of Liquid Crystals, Vol. 1: Fundamentals*; Demus, D., Goodby, J., Gray, G. W., Spiess, H.-W., Vill, V., Eds.; Wiley-VCH: Weinheim, 1998; p 221.
(35) Eelkema, R. Liquid Crystals As Amplifiers Of Molecular Chirality. Ph.D. Thesis, University of Groningen, 2006.
(36) Todd, S. M.; Ferrarini, A.; Moro, G. J. *Phys. Chem. Chem. Phys.* **2001**, *3*, 5535–5541.
(37) The molecular surfaces are generated with MSMS (Sanner, M. F.; Olson, A.; Spehner, J.-C. *Biopolymers* **1996**, *38*, 305–320) and visualized with Geomview (http://www.geom.uiuc.edu/software/download/geomview.html).
(38) (a) Yokoyama, H.; Kobayashi, S.; Kamei, H. *Mol. Cryst. Liq. Cryst.* **1983**, *99*, 39–52. (b) Matveenko, V. N.; Kirsanov, E. A. *Russ. Chem. Rev.* **1986**, *55*, 743–757. (c) Jerôme, B. In *Handbook of Liquid Crystals*; Demus, D., Goodby, J., Gray, G. W., Spiess, H.-W., Vill, V., Eds.; Wiley-VCH: Weinheim, 1998; Vol. 1, p 535.

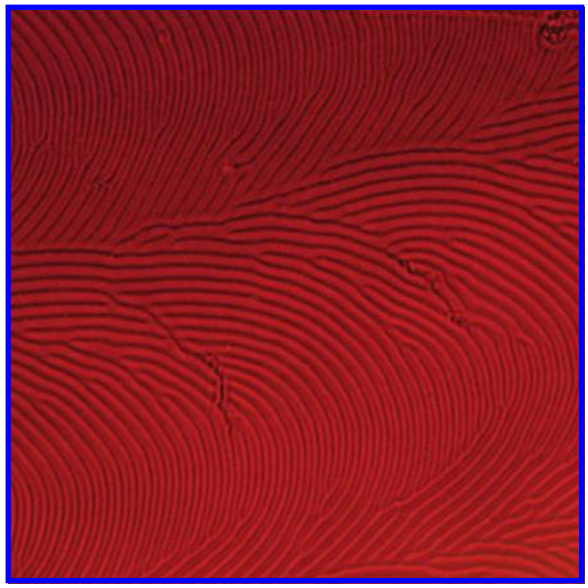

Figure 7. Optical micrograph of the fingerprint texture formed by depositing a droplet of E7 doped with (*P*)-**1a** (1 wt %) on a surface of rubbed polyimide (239 μm × 239 μm). The arched features originate from the variation of thickness along the droplet. Locally, the thickness of the sample is constant and the stripes are parallel.

(0.96 wt %) was deposited on a surface of silanated glass, imposing homeotropic (HH) anchoring.[21] The period of the observed fingerprint texture in this condition is known to depend on the cholesteric pitch as well as on the film thickness.[2b] Under irradiation with UV light, an increase of the fingerprint period was observed, but no rotation was ever detected, which demonstrates that the texture rotation of the doped cholesteric film is directly connected to the hybrid anchoring of the film.

A theoretical analysis based on minimization of the elastic free energy of the system shows that, under hybrid (PH) anchoring, two regions can be distinguished in a cholesteric layer of thickness D, where D is larger than a few times the natural pitch p, defined in eq 11. In most of the sample, a cholesteric helix with pitch $p' \sim p$ is present (we shall call this the *helical layer*); only in a thin *elastic boundary layer* (of thickness d), close to the homeotropic boundary, the director is forced to a strong deformation, to comply with the anchoring condition.[20] The deformation within this layer is characterized by a periodicity Λ, which corresponds to the period of the stripes as observed by optical microscopy, normal to the angle β_0 between the stripes and the director orientation on the substrate, the latter being known from the rubbing direction. A schematic representation of this configuration is shown in Figure 8.

We have calculated the parameters characterizing the director configuration across the doped E7 film, in particular the periodicity Λ of the stripes in the texture, the angle β_0, the pitch p' in the helical layer, and the thickness of the elastic boundary layer d, by minimizing the elastic free energy of the system, eq 10, under the boundary conditions of PH anchoring, according to the model presented in ref 20. In our calculations, we have used the elastic constants reported for pure E7, i.e., $K_{11} = 10.3$ pN, $K_{22} = 7.4$ pN, and $K_{33} = 16.5$ pN ($T = 25$ °C).[21,40] Figure 9 shows the periodicity Λ of the texture modulation and the

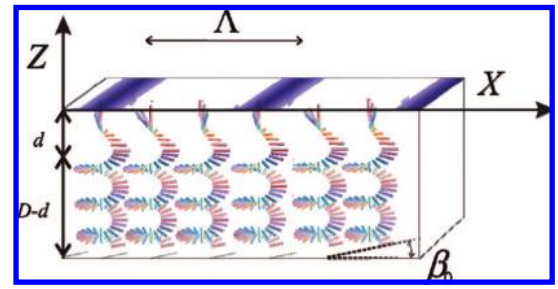

Figure 8. Director configuration across a cholesteric film of constant thickness D with hybrid (PH) anchoring, according to the model presented in ref 20. The rods show the orientation of the director in the film. Λ is the period of the stripes in the fingerprint texture, β_0 is the angle between the normal to these stripes and the orientation of the director on the substrate, and d is the thickness of the elastic boundary layer.

angle β_0, as a function of the ratio D/p. We can see that, over the entire range explored, the periodicity Λ is roughly twice the natural pitch, $\Lambda \approx 2.16p$. This is in agreement with our experimental findings: in the absence of irradiation with UV light, the periodicity of the stripes in the textures of the doped E7 films is close to twice the natural pitch measured for the same system by the Grandjean−Cano method.[2,3] The predicted thickness of the elastic boundary layer, d, is about $0.47p$ and starts increasing only when the thickness D becomes comparable with the natural pitch p; the ratio p'/p in the helical layer is very close to unity and exhibits a smooth decrease with decreasing p. Figure 9 shows that the angle β_0 changes roughly linearly with $1/p$ for a given film thickness: $\beta_0 \approx -\pi + 2\pi D/p$. This reflects the director orientation in the helical layer, starting from the alignment on the substrate defined by the rubbing direction: the bottom being fixed, the number of turns in the helical layer, which is proportional to $(D - d)/p$, imposes the value of β_0.

Dynamics of Reorganization and Analysis of the Texture Rotation. From the analysis presented in the previous sections, the following mechanism can be proposed for the director reorganization in the cholesteric film of E7 doped with **1**. As a consequence of the hybrid (PH) anchoring, the lowest energy configuration of the cholesteric film is helical, with the helix axis perpendicular to the substrate across the whole thickness, except for a thin layer close to the interface with air. In the absence of UV light, the amount of (*M*)-**1b** in the film is negligible; therefore, according to eq 1 with ee = 1 (i.e., 100%), the helical pitch can be expressed as $p \approx c\ \mathrm{HTP}_P$, where HTP_P is the helical twisting power of (*P*)-**1a**. In the presence of light, (*P*)-**1a** → (*M*)-**1b** photoisomerization occurs. From the measured HTP_P, which is positive, and the calculated HTP_M, which is similar in magnitude to HTP_P but negative, the helix is expected to first unwind, to lead to a nematic texture, and then to rewind with opposite handedness, until reaching the PSS. The pitch at the PSS is $p \approx c\ \mathrm{HTP}_{PSS}$, where HTP_{PSS} is determined by the contribution of both isomers, according to eq 2. As p increases at the beginning of illumination, the number of turns in the helical layer decreases, and so β_0, the orientation of the stripes in the texture with respect to the rubbed surface, changes as shown in Figure 9, leading to an overall rotation of the texture. The change of the cholesteric helix from right- to left-handed when the UV light is switched on is accompanied by a clockwise rotation of the texture; the sense of rotation is inverted when, after switching off the light, the right-handed helix is restored.[10,11]

For a complete understanding of the phenomenon, the dynamics of the reorganization process must be considered. This

(39) Meister, R.; Dumoulin, H.; Hallé, M.-A.; Pieranski, P. *J. Phys. Fr. II* **1996**, *6*, 827–844.
(40) Strömer, J. F.; Raynes, E. P.; Brown, C. V. *Appl. Phys. Lett.* **2006**, *88*, 051915/1.

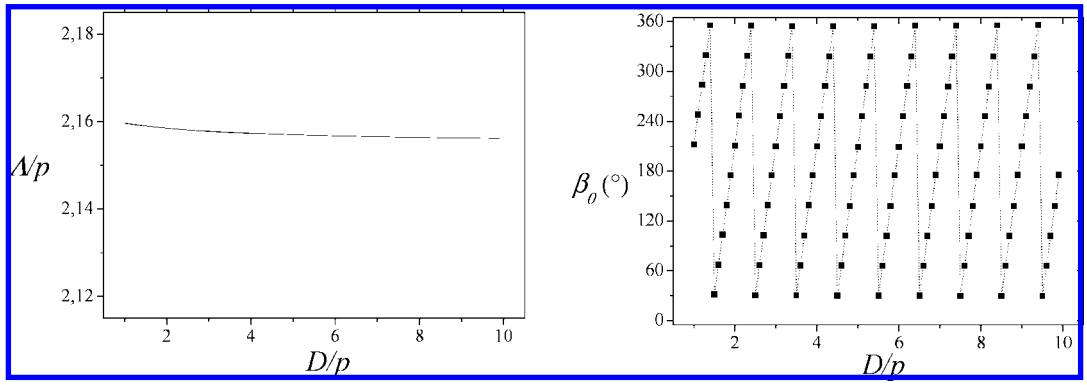

Figure 9. Periodicity Λ of the stripes in the fingerprint texture (left) and angle β_0 between the director orientation on the substrate and the normal to the stripes (right), calculated for a cholesteric film of thickness D and natural pitch p with hybrid (PH) anchoring. The elastic constants reported for E7 in ref 40 have been assumed.

involves slow collective variables, and the methods of nematodynamics should be used to describe the coupling between time evolution of the director and flux of matter in the film.[41] However, if we neglect the role of the thin elastic boundary layer, a useful insight derives from the analysis of a simplified system, i.e., a cholesteric layer with the director strongly anchored parallel to the substrate on one side and free boundary conditions at the opposite interface.[21] The equilibrium configuration of the director in this sample is characterized by a uniform helical twist distortion, with the helix axis perpendicular to the substrate and the pitch defined by eq 11; if the chiral strength is not constant in time, as occurs in the presence of isomerization of the chiral dopant, the director configuration in the film changes with time. Two time scales enter the process: One is determined by material properties of the liquid crystal: the twist viscosity coefficient γ_1 (opposing director rotation)[2] and the twist elastic constant K_{22}. The characteristic time $\tau_{nem} = D^2 \gamma_1/K_{22}$ is of the order of seconds for layer thickness D of the order of micrometers. The other time scale is defined by the isomerization process and can show a wide variability, due to its dependence on the chemical structure of the chiral dopant;[42] we shall call it τ_{isom}, with $\tau_{isom} = \tau_{photo}$ or $\tau_{isom} = \tau_{therm}$, according to whether the isomerization occurs in the presence or absence of UV light. The time evolution of the director reorganization can be described in a very simple way if $\tau_{isom} \gg \tau_{nem}$; in this regime, the process can be seen as helix unwinding under the control of the isomerization process and occurs through a sequence of equilibrium states: at each time, the helical pitch is uniform throughout the film, equal to the value corresponding to the actual concentration of the two interconverting isomers.[21] Using for E7 the values $K_{22} = 7.4$ pN[40] and $\gamma_1 = 0.08$ Pa·s[2b] and giving the thickness D the reasonable value of 20 μm, the time constant $\tau_{nem} = 4$ s is obtained; for isomerization rates of the order of hundreds of seconds, the condition $\tau_{isom} \gg \tau_{nem}$ is satisfied.

Using this simple model for the helical layer of our cholesteric films with hybrid (HP) anchoring, the director reorganization can be described in terms of the time dependence of the cholesteric wavenumber $q = 2\pi/p$, which is related to the isomer composition as

$$q(t) = q_P + (q_M - q_P)x_M(t) \tag{14}$$

where $q_P = 2\pi c\ \mathrm{HTP}_P$ and $q_M = 2\pi c\ \mathrm{HTP}_M$ are the wavenumbers for the (*P*)-**1a** and the (*M*)-**1b** isomers, respectively, at the dopant concentration c, and $x_M(t)$ is the fraction of *M* isomer at time t. According to eq 3b, during the photoisomerization process, starting from the equilibrium state in the absence of UV light, the fraction of *M* isomer can be approximated as $x_M(t) \approx x_{M,PSS}(1 - e^{-t/\tau_{photo}})$, with $x_{M,PSS}$ being the fraction of *M* isomer in the PSS. Then, using the relation found above between the texture periodicity and the cholesteric pitch, we can write

$$\Lambda(t) \approx 2.16p(t) \approx \frac{2.16}{c}\,\frac{1}{\mathrm{HTP}_P + (\mathrm{HTP}_M - \mathrm{HTP}_P)x_{M,PSS}(1 - e^{-t/\tau_{photo}})} \tag{15}$$

Analogously, taking into account the inverse proportionality between the angle β_0 and the pitch p, shown in Figure 9, we can write

$$\beta_0(t) \sim -\pi + 2\pi cD[\mathrm{HTP}_P + (\mathrm{HTP}_M - \mathrm{HTP}_P)x_{M,PSS}(1 - e^{-t/\tau_{photo}})] \tag{16}$$

Equations 15 and 16 have been used to analyze the time evolution, under irradiation, of the textures of two semifree cholesteric films of E7, both doped with **1** (1 wt %) and deposited on rubbed polyimide, but having *a priori* different thicknesses. In case A, the stripes constituting the fingerprint texture disappeared after more than 150 s of irradiation, whereas in case B, this took slightly more than 60 s. The same lamp was used in the two experiments; however, the distance and angle of the lamp with respect to the sample were not rigorously the same. Experimental data have been analyzed on areas of constant thickness so as to extract the curves $\Lambda(t)$ and $\beta_0(t)$. These curves have been compared to eqs 15 and 16, where the helical twisting power of the (*P*)-**1a** isomer has been taken equal to that measured in the absence of irradiation, $\mathrm{HTP}_P = 90$ $\mu\mathrm{m}^{-1}$,[9] whereas for the (*M*)-**1b** isomer $\mathrm{HTP}_M \sim -\mathrm{HTP}_P$ has been assumed, as obtained from calculations with the surface interaction model. The fraction of (*M*)-**1b** isomer in the PSS has been given the value $x_{M,PSS} = 0.9$. The characteristic time τ_{photo} and the film thickness D are derived from comparison between experiment and theoretical predictions. The results are presented in Figure 10. We can see that the time dependence of the stripe periodicity is similar in cases A and B, at least at the beginning of irradiation, with some more differences appearing at longer times. Such behavior can be explained considering that, under the same conditions of irradiation, the isomerization process occurs at the same rate and, with identical

(41) (a) Leslie, F. M. *Q. J. Mech. Appl. Math.* **1966**, *19*, 357–370. (b) Ericksen, J. L. *Arch. Ration. Mech. Analysis* **1960**, *4*, 231–237.
(42) Pollard, M. M.; Klok, M.; Pijper, D.; Feringa, B. L. *Adv. Funct. Mat.* **2007**, *17*, 718–729.

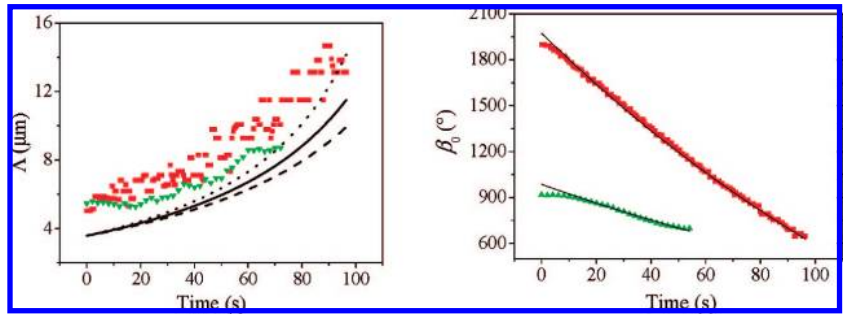

Figure 10. (Left) Periodicity of the stripes in the texture, Λ, as function of time, as obtained by UV irradiation of two semifree cholesteric films of E7 doped with **1** (1 wt %), deposited on rubbed polyimide. Red squares and green triangles are used for two different films, denoted as A and B, respectively. The curves have been calculated according to eq 15, with $\tau_{photo} = 180$ (dotted line), 200 (solid line), and 220 s (dashed line). (Right) On the same samples, time dependence of the angle β_0 between the normal to the stripes and the anchoring direction on the substrate, modified by an arbitrary phase shift. The theoretical curves (solid line) have been obtained from eq 16, with $\tau_{photo} = 200$ s and $D = 9$ μm (A) or $D = 3.3$ μm (B).

dopant concentration, the natural pitch changes in the same way in the two films. As a consequence, also the stripe periodicity is expected to be the same, at least as long as the film thickness remains large enough compared to the natural pitch of the cholesteric LC. The disappearance of the fingerprint texture indicates that this is no longer true at the end of experiment B, and this is probably the reason for the increasing differences with time between the data collected in experiments A and B.

We can see in Figure 10 that, in both cases, the measured periodicity in the absence of UV light ($t = 0$) is about 20% higher than the theoretical prediction, $\Lambda(0) \approx 2.16p_P$. The real significance of this difference is difficult to assess, due to the error affecting the measured periodicity and the uncertainty in the parameters used in eq 15: the fraction of (*M*)-**1b** isomer in the PSS state, $x_{M,PSS}$, the experimental value of HTP_P (with an error of the order of 5−10%), and the elastic constants used for E7.[40] However, this difference could also be associated with the approximation of the model that we have used to describe the director configuration, which ignores the corrugation of the LC−air interface. Actually, topographic modulations at the air interface have been evidenced by atomic force microscopy at the surface of the semifree cholesteric film.[10,11,43] The possible influence of surface height modulations will be addressed in future investigations.

Figure 10 shows the curves calculated with eq 15 and $\tau_{photo} = 180$, 200, and 220 s. A precise determination of the characteristic time τ_{photo} is not possible; a general underestimate of the texture periodicity is obtained with $\tau_{photo} = 200$ s, which however reproduces the slope of the experimental curve. This value is in line with the estimate of hundreds of seconds, obtained from the considerations on the isomerization kinetics, reported in a previous section. From comparison with the thermal isomerization rate, $\tau_{therm} > 10^3$ s, a sizable slowing down of the rotation of the texture modulation is expected in the absence of UV light. Indeed, in our experiments we found that the recovery of the thermal equilibrium state, after switching off the UV light, was 5−6 times slower than the process leading to the PSS under UV irradiation.

The plot on the right-hand side of Figure 10 shows that, if the initial very short transient is neglected, the angle $\beta_0(t)$ exhibits a monotonic decrease with time, in keeping with the prediction of the model presented above for the reorganization of the director under the control of the isomerization kinetics. The narrower range of β_0 values in experiment B reflects a lower number of turns required to unwind the cholesteric helix, due to a smaller thickness of the film. The theoretical curves have been calculated using eq 16 with $\tau_{photo} = 200$ s, providing the following values for the film thickness: $D = 9$ μm for experiment A and $D = 3.3$ μm for experiment B (both involve a dopant concentration of 1 wt %). In experiment A, the calculated thickness is modified from about 5 times the cholesteric pitch in the absence of UV irradiation to less than 2 times the pitch after 100 s of UV irradiation. In experiment B, this thickness changes from about twice the pitch before irradiation to a single pitch after 50 s of UV irradiation. This calculated value is in agreement with the observed disappearance of the fingerprint after 50 s of UV irradiation.

Conclusions

A joint theoretical and experimental investigation has allowed us to unveil the mechanism of the recently observed photoinduced rotational reorganization of semifree cholesteric liquid crystal films.[10,11] Now we can give a complete description of the phenomenon, where the role of each contribution is clearly identified and quantitative estimates are provided. Modeling enables us to rationalize the orientational behavior of the chiral dopant and its twisting ability. Under irradiation, isomerization of the chiral dopant occurs. The two isomers of **1**, characterized by opposite values of the dihedral angle between the fluorene and the naphthyl moiety, orient in a similar way in the LC host, with the fluorene plane preferentially parallel to the local director. As a consequence of their shape and their average alignment, the two isomers impart oppositely handed helicity to the phase; they have high HTP, very close in magnitude and opposite in sign, and therefore a large difference in HTP, leading to a rapid evolution of the cholesteric pitch under irradiation as the concentration of the two isomers varies. This feature is of utmost relevance for the occurrence of huge and relatively fast rotational reorganization.

We have also shown that the texture modulation rotation observed under irradiation derives from unwinding of the cholesteric helix, which is produced by the photoisomerization of the chiral dopant; as the concentration of the two isomers changes, the pitch is adjusted and the director rotates so as to minimize the elastic free energy. The rotation appears intimately related to the hybrid (PH) anchoring of the cholesteric film, planar on the rubbed polymer and homeotropic at air, leading to strong deformation of the cholesteric helix close to the LC−air interface to comply with the homeotropic anchoring.

(43) (a) Meister, R.; Hallé, M.-A.; Dumoulin, H.; Pieranski, P. *Phys. Rev. E* **1996**, *54*, 3771–3782. (b) Boudet, A.; Mitov, M.; Bourgerette, C.; Ondarçuhu, T.; Coratger, R. *Ultramicroscopy* **2001**, *88*, 219–229.

These deformations correspond to the formation of a structure with stripes visible by optical microscopy. The relationship between the orientation of this texture modulation and the number of helical turns in the film finally appears to determine the characteristics of the texture rotation under irradiation.

The sense of rotation depends on the HTP difference between the two isomers of the chiral dopant. Helix unwinding is accompanied by a change in the periodicity and rotation of the texture modulation. Flux of matter might be present, e.g., in the region of the film close to the LC−air interface; however, it does not need to be invoked to explain the microscopy observations. Defects also do not seem to play a significant role, in contrast with what was originally hypothesized.[10]

Different time scales can be distinguished: the director reorientation falls in the second range, whereas the rates of the isomerization processes depend on the exact chemical structure of the chiral dopant. We have shown that, if the isomerization time is longer than tens of seconds, the film reorganization occurs under its control, through a sequence of equilibrium states, each characterized by a practically uniform cholesteric helix throughout the whole film, with its pitch scarcely affected by the boundary constraints. The reorganization is reversible, as is the isomerization of the dopant, but is slower in the absence of irradiation with UV light (thermally) than under irradiation; this simply reflects the rate of the isomerization process which, due to the availability of the faster photochemical pathway, increases with the irradiation power. The phenomenon has a thermodynamic origin: the driving force is the elastic free energy change produced by the change of HTP with isomerization. Accordingly, its rate depends upon the isomerization rate and the HTP difference between the interconverting isomers. A direct mechanical effect of the motor molecules on the LC host must be excluded.

We are now able to summarize how both the characteristics of the chiral switchable dopant and the properties of the LC host determine the rotational reorganization of the film. The characteristics of the LC−air interface, and thus the possibility of observing the texture rotation, should depend on the chemical structure of the nematic mesogens. We expect that the phenomenon should be more generally observed for nematics with longitudinal electric dipole, i.e., with a positive dielectric anisotropy. Both dopant and host influence the thermal isomerization rate, since the friction opposing the rearrangement of the motor in the LC host depends on the molecular shape and the viscosity of the environment, according to the Kramers theory for activated processes. Scarce information is available on the viscosity experienced by a dopant in the LC medium; however, we do not expect that the choice of the nematic solvent should have dramatic effects on the isomerization rate. On the contrary, the design of the chiral switchable dopant is crucial: even small structural changes can drastically affect the energetic and dynamic features of the isomerization process, as well as the HTP of these chiral dopants.[11,41] The optical properties of these dopants also influence the rotation, in determining the ratio between photo- and thermal isomerization rates. To conclude, spectacular macroscopic effects such as those reported in refs10 and11 can be controlled by meeting specific requirements for the geometry of the experiment and by adapting the structure of both the nematic LC host and the switchable chiral dopant.

Acknowledgment. Linear dichroism spectra were recorded by B. Serrano Ramon, under the supervision of Prof. D. J. Broer (Eindhoven University of Technology), for which they are gratefully acknowledged. Dr. J. Salomon (Université Paris Dauphine) is acknowledged for his help with developing the Matlab routine for analysis of textures. M. Walko is acknowledged for having carried out initial DFT calculations on motor molecule **1**. S. Akamatsu is acknowledged for the supply of an optical microscope and a camera. This work was supported by grants from MIUR-PRIN 2005 (A.B. and A.F.), by The Netherlands Organization for Scientific Research (NWO-CW) via a Veni Grant (N.K.), and by NanoNed (M.G.M.J).

Supporting Information Available: Description of experiments and details of calculations. This material is available free of charge via the Internet at http://pubs.acs.org.

JA8039629